T. Hong, F. De Leon and Q. Zhu, Optimal Dispatch of Electric Transmission System Considering Interdependencies with Natural Gas Systems," Game Theory for Security Risk Management, Static & Dynamic Game Theory Series, Birkhauser, 2018.

Optimal Dispatch of Electric Transmission Systems Considering Interdependencies with Natural Gas Systems

Tianqi Hong, Francisco de León, and Quanyan Zhu

[1] Tianqi Hong, New York University, 5 Metrotech Center, Brooklyn, NY, Email: th1275@nyu.edu
[2] Francisco de León, New York University, 5 Metrotech Center, Brooklyn, NY, Email: fdeleon@nyu.edu
[3] Quanyan Zhu, New York University, 5 Metrotech Center, Brooklyn, NY, Email: quanyan.zhu@nyu.edu

Summary. This paper presents a novel model to assess the interdependencies between electric power systems interconnected with natural gas systems. The impact from natural gas systems in the electric power system can be evaluated with the proposed model in normal operation and contingency situations. To reduce the impact of interdependencies, additional constraints to the optimal dispatch problem are formulated. The interdependency constraints can be integrated into the normal optimal power flow problem and security-constrained optimal power flow problem to improve the robustness of the electrical power system. A co-simulation platform is built in Matlab environment. We evaluate the proposed model using the IEEE 14-bus system and a corresponding natural gas transmission system. According to the simulation results, the reliability of the power system is improved when interdependency constraints are considered.

1 Introduction

Early in the 20th century the fundamental models for major civil infrastructures were developed and are now well-established. However, most of the managers still plan and operate of their infrastructures individually even when those systems are physically interconnected. In the past decades, engineers in different areas devoted themselves to decouple the interdependencies between different infrastructures. Interdependencies have been reduced but not eliminated. Frequently, when one type of interdependency is reduced, other or several other interdependencies are introduced. Perhaps it is now, in the era of the smart grid (and smart everything), the time to stop eliminating the interdependencies between different infrastructures. Rather, one should be thinking about how to manage the response of the system of systems, including interconnected infrastructures in the analysis and optimization.

As the central link between different systems, electric power systems are customers and/or suppliers to other infrastructures. A robust electric power system is a prerequisite to improve the reliability of the combined system. Hence, enhancing the reliability of the electric power system by considering the interdependency impact (IDI) coming from other interconnected systems is necessary. In this paper, we focus on the study of interconnected electric natural gas (ENG) system. Fig.1 illustrates the structure of an example ENG system. Previous researchers have noticed the critical nature of the electric power system and investigated the interdependencies between the electric power and natural gas systems [1, 2, 3, 4]. In references [2, 3, 4], a unified model was established to model the coupled ENG system in normal operation by considering their interdependency. Instead of modeling the interdependencies, some researchers introduced the concept of energy hub [5, 6, 7]. They proposed several methods under different scenarios to allocate the energy hub and reduce the operational cost for the coupled system. Uncertainties, such as human activities, of the combined system are considered in [2, 8, 9, 10].

Instead of the interdependency impact (IDI) in normal operating condition, some groups have also put their efforts in modeling and analyzing the post-contingency interdependency impacts (PCIDIs) in the coupled networks. The authors of [10, 11, 12] have proposed various formulations to reduce the PCIDIs and improve the robustness of the joint systems.

All of the previous studies assume that their linked system is working under a co-dispatch operation scheme, meaning the utilities of the natural gas and electrical power systems share their information and operate their systems together. In practice, this assumption may not be true for two reasons: First, the operational time scales of natural gas and electric power systems are quite different. Electric power systems can be dispatched every hour. In contrast, natural gas systems are normally dispatched on a period of several days. Second, only limited data can be shared between different utilities or departments for security reasons. To assess the IDIs with the limitations aforementioned, different models and solutions for enhancing the robustness of the electric power system are investigated in this paper.

The original contributions of this paper are: (a) a detailed natural gas flow model is proposed for the evaluation of the IDIs from the natural gas transmission system. We model

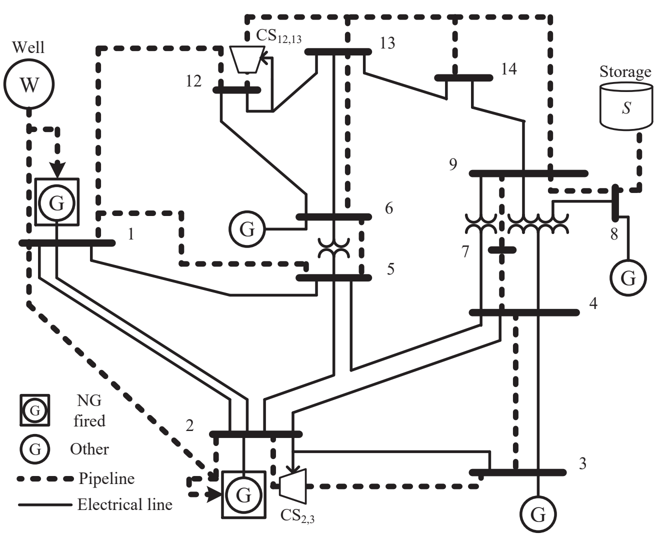

Fig. 1. Structure of the electric-natural gas system

natural gas flow with long transmission pipelines (medium length for electrical lines); (b) a decentralized operating pattern with limited data exchanges between the natural gas and electrical transmission systems is analyzed; (c) several novel constraints for the integration of the PCIDIs into the electric power system are proposed and evaluated, for example: interdependency with compressor stations and gas-fired generation; and (d) the corresponding solution is provided.

2 Modelling of Natural Gas Transmission System

A natural gas system can be considered both a customer and a supplier of the interconnected electrical power system. As a supplier, the natural gas system provides fuel to power plants to generate electricity. As a customer, the natural gas system consumes electricity that powers the pressure pumps. This interdependent relationship benefits each other and may cause instability on both systems. In this paper, we only concentrate on reducing IDIs to the electrical power system. To develop a physical model representing the IDIs generated by the natural gas system, we first establish a physical model of the natural gas system.

2.1 Physical Relationships of Natural Gas Transmission Systems

Different from [2] to [12], the Panhandle A equation is chosen to model the relationship between natural gas flow rate and pressure drops. The Panhandle A equation has higher accuracy than other equations for systems with large pressure drops. The natural gas flow rate from node k to node m (F_{km}) in steady state is given by [13]:

$$F_{km} = A_{km}^{NG}\left[|r_{km}^2 p_k^2 - r_{mk}^2 p_m^2|\right]^{0.5394}, \tag{1}$$

where:

$$A_{km}^{NG} = \frac{4.5965\times 10^{-3}\eta_{km}^{p} D_{km}^{2.6182}}{sign(p_k - pr_m)(G^{0.854}T^f L_{km} Z_{km})^{0.5394}}\left(\frac{T^b}{p^b}\right). \tag{2}$$

F_{km} is the flow rate of pipeline km in $\mathrm{m}^3/\mathrm{day}$; r_{km} is the compression ratio of pipeline km at node k; p_k and p^b are the pressure at node k and base pressure in kPa; D_{km} is the inside diameter in mm; L_{km} is the length of the pipe in km; Z_{km} is the compressibility factors of pipeline km; ${}^{p}_{km}$ is the efficiency of the pipeline; T^f and T^b are the average gas flow temperature and base temperature in K; G is the specific gravity of the gas delivered by pipeline; sign(x) is a function to extract the sign of variable x.

Compressor stations are important elements for compensating the pressure drop in the natural gas transmission system. Centrifugal and positive displacement compressors are the most commonly used. By converting electric power into mechanical power, the compressor station is a critical link between the electrical and natural gas systems, especially at the transmission level. The relationship between the electric power and compression ratio is given in [13] as:

$$P_{km}^{E} = \frac{Z_k + Z_m}{2\eta_{km}^{c}}\left(\frac{\gamma}{\gamma-1}\right)\frac{4.0639 F_{km} T^s}{10^6}\left[(r_{km})^{\frac{\gamma-1}{\gamma}} - 1\right]. \tag{3}$$

where P_{km}^{E} is the electric power consumption of compressor at pipeline km in kW; Z_k is the compressibility factors at node k; ${}^{p}_{km}$ is the efficiency of the compressor station; T^k is the temperature at node k; γ is the ratio of specific heats of gas according to [13], γ is 1.4 for natural gas. Based on (3), the electrical power consumption P^E_{km} has direct relationships with flow rate F_{km} and compression ratio r_{km}. The electric power consumption changes when the flow rate F_{km} or compression ratio $r_k m$ changes.

Based on (3), the electrical power consumption P^E_{km} has direct relationships with flow rate F_{km} and compression ratio r_{km}. The electric power consumption changes when the flow rate F_{km} or compression ratio r_{km} changes.

Natural gas fired generators are other links between natural gas systems and electric power systems. Since all generators are equipped with an automatic generation controller (AGC), the flow rate consumption of the generators is constant.

Similar to the nodal constraints in the electrical power system, the summation of the gas flow rate at each node must be zero at all times. Therefore, we arrive at:

$$F^I_{km} = F^D_{km} + \sum_{\substack{m=1 \\ m \neq k}}^{NN} F_{km}, \tag{4}$$

where F^I_k and F^D_k are the flow rates of the injection and demand of node k.

2.2 Modeling the Natural Gas System under Normal Operation

In normal operation, managers of a natural gas transmission company expect to operate their systems efficiently. To reduce the operational costs and improve the total efficiency of a natural gas transmission system, the gas dispatch becomes as an optimization problem.

The dispatchable parameters in the natural gas systems can be clustered in three types. The first variable is the pressure of the source. The natural gas source is normally considered the gas plant or large gas storage where its pressure can be kept constant and its capacity is assumed to be infinity; see the natural gas well in Fig.1. The second variable is the flow rate of short-term storage. Since the manager can dispatch the flow rate of a short-term storage to improve the performance of the system, the terminal pressure of the storage varies according to the working status of the natural gas system. Naturally, the gas price of short-term storage is higher than that of a natural gas well. Thus, the flow rates from a natural gas source and short-term storage can be considered flow injections with different prices. The third variable is the compression ratio of each station. Compressor stations can regulate the flow rate or terminal pressures of a pipeline by adjusting the compression ratio. Note that the compressor station allocation problem is beyond the scope of this paper.

Considering the dispatchable parameters discussed above, an optimal natural gas flow (ONGF) problem can be formulated as:

$$\min_{\mathbf{p}^w, \mathbf{F}^I, \mathbf{r}} M^{NG} = \min_{\mathbf{p}^w, \mathbf{F}^I, \mathbf{r}} \sum_{k=1}^{NN} \left(C^{NG}_k F^I_k + C^E_k \sum_{m}^{NP} P^E_{km} \right), \tag{5}$$

where $\mathbf{F}^I$ is a column vector consisting of the flow rate injection at each node, $\mathbf{r}$ is a column vector consisting of compressor station ratios, $\mathbf{p}^w$ is a column vector consisting the pressure of the natural gas well, C^{NG}_k is the price of natural gas at node k in \$/Mm^3/s, C^E_k is the price of electricity at node k in \$/MW/s.

The equality constraints of problem (5) are the flow rate nodal constraints presented in (4). The major inequality operation constraints of a natural gas transmission system are to keep pressures, flow rates and injections, within limits. These are expressed mathematically as:

$$\underline{p_k} \leq p_k \leq \overline{p_k}, \tag{6}$$

$$\underline{F_{km}} \leq p_k \leq \overline{F_{km}}, \tag{7}$$

$$\underline{F_k^I} \leq F_k^I \leq \overline{F_k^I}, \tag{8}$$

where $\bar{x}$ and $\underline{x}$ are the upper and lower bounds of variable x.

The lower and upper bounds of the natural gas pipeline flow are calculated according to the erosional velocity of each pipeline. The erosional velocity $\overline{\mu_{km,k}}$ of the pipeline km with reference to the node k is (isothermal flow) [13]:

$$\overline{\mu_{km,k}} = 100\sqrt{\frac{Z_k R(T_k + 460)}{199.96 p_k G}}, \tag{9}$$

where $\overline{\mu_{km,k}}$ is in the unit of m/s, R is a constant that equals to 8.314 J/K/mol, Z_k is the compressibility factor at node k. The relationship between the maximum velocity and upper bound of the flow rate can be described as [13]:

$$\overline{F_{km}} = \min\left\{\overline{F_{km,k}}, \overline{F_{km,m}}\right\}, \tag{10}$$

where

$$\overline{F_{km,x}} = \left(\frac{D_{km}^2 \overline{\mu_{km,x}}}{14.7349}\right)\left(\frac{T_b}{p_b}\right)\left(\frac{\overline{p_x}}{Z_x}\right)\Bigg|_{x=k,m}. \tag{11}$$

To solve the non-convex optimization problem (5), some simplifications have been made as follows:

(1) The compressibility factor Z at each bus is considered to be a constant value ($Z = 0.9$ for the natural gas [13], p. 67);

(2) The inner temperature at each node is considered to be constant (T_k = 20 + 273 K);

(3) All natural gas pipelines are considered in a horizontal placement, therefore removing the gravity effect.

The simplifications listed above are used to reduce the computational complexity of solving natural gas flow problems, which remains very general and believed to be more accurate than existing formulations.

Problem (5) can be solved using the Primal-Dual Interior Point Algorithm (PDIPA) with truncated Newton step. The convergence of PDIPA is ensured and the first order optimality conditions can be satisfied [14, 15, 16]. Normally, a current working status of natural gas transmission systems can be used as a feasible initial point for the ONGF problem. It is worth noting that the final solution may not be the global optimum due to the non-convexity of the original ONGF problem.

After obtaining the solution of the ONGF problem, the electricity consumption of each compressor station in normal operation can be obtained from (3). We can then construct a column vector $\mathbf{e}_{(0)}$ to represent the normal electricity consumption as:

$$\mathbf{e}_{(0)} = \left[P_1^E, \ldots, P_{NN}^E\right], \tag{12}$$

where

$$P_k^E = \sum_{\substack{m=1 \\ m \neq k}}^{NN} P_{km}^E. \tag{13}$$

2.3 Modeling the Natural Gas System under Contingency

Since the combined systems are operated independently, we assume that the two systems cannot communicate with each other frequently. Additionally, the operational time scales of the two systems are different and the electrical power system cannot estimate when the PCIDI hits the electrical system. Hence, it is essential to consider the worst post-contingency impact of the natural gas system in the operation of the electrical system.

In pre-contingency scenarios, the natural gas system operates based on the ONGF results discussed in Section 2.2. When a contingency occurs, the pressures of each node and the flow rates of each pipeline may change. Consequently, the electrical consumptions of the compressors will change. Since generators are modeled as the customers of the natural gas system with constant flow rate demands, the natural gas system needs to satisfy the requirements from the connected generators unless the pressures of the nodes are reduced below certain limits. As a result, the impacts on the electrical system come from the electricity demand variations and the loss of generators regardless on how the natural gas system is dispatched. This is true for the original dispatch or re-dispatch after contingency. Hence, the worst PCIDI can be obtained through an exhaustive "what if" analysis.

In normal condition, the natural gas system is dispatched according to the solution of problem (5). For all the possible contingency scenarios, the pressure at each generator is checked to build the pre indicator matrix D^{pr}, where $d^{pr}_{(k)(j)}$ is the $(k,j)^{th}$ element in matrix D^{pr}. Element $d^{pr}_{(k)(j)} = 1$ means the generator at node k needs to be disconnected from natural gas system when the j^{th} contingency occurs. The consumption impact of each compressor station is recorded to form a pre consumption impact matrix E^{pr} where $\mathbf{e}^{pr}_{(j)} - \mathbf{e}_{(0)}$ is the j^{th} column of the matrix E^{pr}. Vector $\mathbf{e}^{pr}_{(j)}$ can be built based on (12) under the j^{th} contingency. Then,

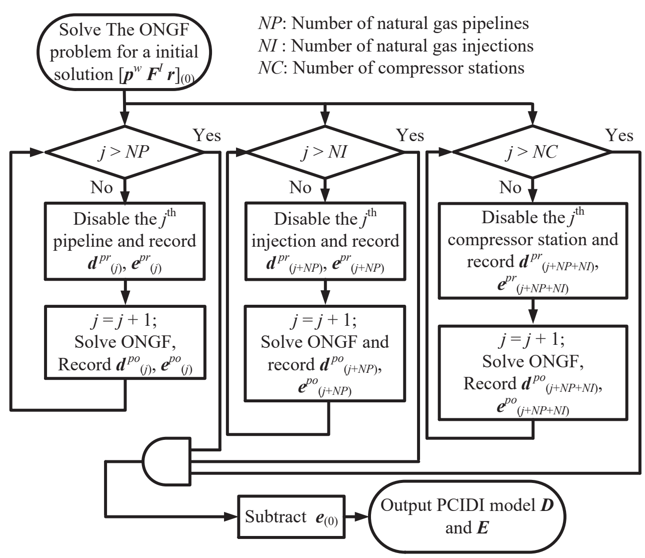

Fig. 2. Flowchart of "what if" analysis

we assume that the natural gas system would be re-dispatched according to the solution of (5) with the natural gas system in post-contingency configuration. Similarly, a post indicator matrix D^{po} and post electrical consumption matrix E^{po} can be constructed. Fig. 2 shows the flowchart of the proposed "what if" analysis. All the matrixes can be built a day-ahead or online according to load profiles.

Note that the electrical consumption of the compressor station changes regardless of whether the natural gas system is dispatched based on the security-constrained optimal natural gas flow [12] or just optimal natural gas flow, since the natural gas flow rate in (3) would change depending on the system operating status. Current literature has ignored this critical PCIDI between the natural gas system and the electrical power system.

Matrixes $D = [D^{pr}, D^{po}]$ and $E = [E^{pr}, E^{po}]$ are the interdependency impact model to the electrical power system. To protect the network data of natural gas systems, the gas utilities can build all the matrixes and only share numerical matrixes with electric power utilities.

3 Electric Power System Modeling

After the IDI model has been obtained from the natural gas system, the IDIs on the electric power system needs to be solved. Hence, a set of interdependency constraints is formulated in this section. The interdependency constraints provide a tool to integrate the impact into the power system dispatch analysis. To illustrate this, we start from the traditional formulation of OPF problem.

3.1 Traditional Optimal Power Flow and Sensitivity Factors

To reduce the operational cost of the electrical transmission system, the power injections should be optimally dispatched. The classic operational cost of the electrical transmission system is defined as [15]:

$$M^E = \sum_{i=1}^{N_B} \left[a_i^E \left(P_i^G \right)^2 + b_i^E P_i^G + c_i^E \right]. \tag{14}$$

where P_i^G is the active power of generator at bus i; a_i^E, b_i^E, and c_i^E are the cost coefficients of the thermal generator at bus i.

According to [15] and [16], the optimal power flow problem can be formulated as:

$$\min_{\mathbf{P}^G, \mathbf{Q}^G} M^E \tag{15}$$

subject to:

$$P_i^G - P_i^D = P_i \tag{16}$$

$$Q_i^G - Q_i^D = Q_i, \tag{17}$$

$$\underline{V_i} \leq V_i \leq \overline{V_i}, \tag{18}$$

$$\underline{I_{ij}} \leq I_{ij} \leq \overline{I_{ij}}, \tag{19}$$

$$\left[\underline{P_i^G}, \underline{Q_i^G} \right] \leq \left[P_i^G, Q_i^G \right] \leq \left[\overline{P_i^G}, \overline{Q_i^G} \right], \tag{20}$$

where $\mathbf{P}^G$ and $\mathbf{Q}^G$ are the decision column vector generated by sequences $\left(P_i^G\right)_i^{N_B}$ and $\left(Q_i^G\right)_i^{N_B}$; P_i^D and Q_i^D are the active and reactive demand at bus i; V_i is the voltage at bus i; I_{ij} is the current of the line ij.

Apart from looking for an economic optimal dispatch solution to achieve minimal operational cost, most utilities also want to improve the reliability of their systems, i.e., to increase the robustness of their system and satisfy the $n-1$ contingency criterion. Hence, the security-constrained optimal power flow (SCOPF) is proposed [15, 17, 18].

The sensitivity factors are the major tools for solving the SCOPF problem. The fundamental sensitivity factors are the power transfer distribution factor (PTDF) [16, 19]. The PTDF is a sensitivity matrix. Element J_{ik}^P in the PTDF describes the change of the active power flow in transmission line i when there is a change of power injection at bus k. According to [16], the element J_{ik}^P is calculated with the dc power flow as:

$$J_{ik}^P = \frac{1}{X_i}\left(\frac{d\theta_{i:1}}{dP_k} - \frac{d\theta_{i:2}}{dP_k}\right), \tag{21}$$

where X_i is the reactance of transmission line i, $\theta_{i:1}$ and $\theta_{i:2}$ are the angles of the from-bus $i:1$ and to-bus $i:2$ of the line i respectively. In matrix form, we have:

$$\Delta\mathbf{a}^G = PTDF \cdot \Delta\mathbf{P}_G, \tag{22}$$

where $\Delta\mathbf{a}^G$ is a column vector representing the linearized change of active power flow of each transmission line induced by generator outage, $\Delta\mathbf{P}_G$ is a column vector representing the changing of active power injection at each bus.

The PTDF can be used to indicate the post contingency status of generator outages in a given electric system. To indicate a line outage scenario, a line outage distribution factor matrix (LODF) is developed [20]. The element J_{ij}^L in the LODF describes the change of the active flow in transmission line i when there is a change of active power flow of transmission line j. The element J_{ij}^L is calculated as [20]:

$$J_{ij}^L = \begin{cases} \left.\frac{J_{i,j:2}^P}{1-J_{j,j:2}^P}\right|_{i\neq j} \\ -1|_{i=j} \end{cases}, \tag{23}$$

where $J_{i,j:2}^P$ is the sensitivity of active power flow in line i with respect to the injection at the to-bus $j:2$ of line j, which can be found in the PTDF matrix. For each scenario of the electric system, a new constraint can be generated based on PTDF and LODF. By incorporating all scenario constraints into problem (14), a classic model of SCOPF problem can be obtained [18].

3.2 Integration of the Interdependency Model into the Power Dispatch Problem

According to (21), the PTDF matrix can be utilized for the estimation of system impacts from changes in power injections. The changes of a load can be seen as a negative power injection. Hence, substituting $\Delta\mathbf{P}_G$ by the impact $\Delta\mathbf{e}_{(j)}^{NG}$ obtained from Section 2.3, the linearized active power flow impact of all the electrical transmission lines can be computed from:

$$\mathbf{a}_{(j)}^{NG} = \mathbf{a}_{(0)} + \Delta\mathbf{a}_{(j)}^{NG} = \mathbf{a}_{(0)} + PTDF \cdot \Delta\mathbf{e}_{(j)}^{NG}, \tag{24}$$

where $\mathbf{a}_{(j)}^{NG}$ is a column vector representing the IDI of active power flows under the j^{th} scenario in the natural gas system, $\mathbf{a}_{(0)}$ is column vector of the active power flows in normal operation and $\Delta\mathbf{e}_{(j)}^{NG}$ is the j^{th} column vector in matrix $\mathbf{E}$.

The PCIDI of the natural gas fired generators can be obtained similarly:

$$\mathbf{P}_{(j)}^{G} = -\mathbf{P}_{(0)}^{G} \cdot \mathbf{d}_{(j)}^{NG}, \tag{25}$$

where $\mathbf{P}_{(j)}^{G}$ is a column vector representing the PCIDI of all the generator outputs under j^{th} scenario in the natural gas system, $\mathbf{P}_{(0)}^{G}$ is column vector of all the generator outputs in normal operation and $\mathbf{d}_{(j)}^{NG}$ is the j_{th} column vector in matrix $\mathbf{D}$.

The PCIDI of the currents in each transmission line can be modelled according to LODF factor:

$$\mathbf{I}_{(j)}^{NG} = \mathbf{I}_{(0)} + \Delta\mathbf{I}_{(j)}^{NG} = \mathbf{I}_{(0)} + LODF \cdot \begin{bmatrix} \Delta\mathbf{a}_{(j)}^{NG} \\ \mathbf{P}_{(j)}^{G} \end{bmatrix}, \tag{26}$$

where $\mathbf{I}_{(j)}^{NG}$ is the column vector corresponding to the impact of the current of the j^{th} scenario in the natural gas system, $\mathbf{I}_{(0)}$ is a column vector of all the currents in normal operation. Comparing $\mathbf{I}_{(j)}^{NG}$ with the upper bound limit of current $\bar{\mathbf{I}}$, the interdependency constraints of the line currents can be obtained from:

$$|I| \leq \begin{cases} \bar{\mathbf{I}}+(\bar{\mathbf{I}}-\mathbf{I}_{(j)}^{NG}) & if\ \bar{\mathbf{I}}-\mathbf{I}_{(j)}^{NG}<0 \\ \bar{\mathbf{I}} & else \end{cases} \qquad \forall j, \tag{27}$$

where I is a column vector constructed from the I_{ij}. The repeated current constraints in (19), SCOPF and (27) are removed and the number of the constraints can be reduced. The line current constraints are ensured by the ac power flow.

The PCIDIs also affect the voltage profile of the electric system. To evaluate this type of impacts, the Jacobian matrix JE of the Newton power flow is introduced. According to [21], we have:

$$\begin{bmatrix} \Delta\mathbf{P} \\ \Delta\mathbf{Q} \end{bmatrix} = \mathbf{J}^{E} \begin{bmatrix} \Delta\theta \\ \Delta\mathbf{V} \end{bmatrix}, \tag{28}$$

Based on matrix E built in Section 2.3, $\Delta\mathbf{Q}$ equals zero. Thus, the $\Delta\mathbf{V}$ can be solved from (28):

$$\Delta\mathbf{V} = \mathbf{H}^{VP}\Delta\mathbf{P}. \tag{29}$$

where $\mathbf{H}^{VP}$ is a sub-matrix obtained from the inverse of Jacobian matrix $\mathbf{J}^{E}$. According to (29), the voltage constraints generated by a natural gas contingency can be described as:

$$\underline{\mathbf{V}} \leq \mathbf{V}_{(0)} + \mathbf{H}^{VP}\Delta\mathbf{a}_{(j)}^{NG} \leq \overline{\mathbf{V}}, \tag{30}$$

where $\mathbf{V}_{(0)}$ is the vector of voltage at each bus of OPF results. By integrating the interdependency constraints of the line current (27) and voltage profile (30) into either the OPF problem or SCOPF problem, a more robust dispatch solution can be obtained; see the flowchart in Fig.3. It is worth pointing out that one can easily implement the proposed impact constraints into other types of OPF problems. Instead of replacing the original method, the proposed tool provides a new view for the operator to dispatch the system.

4 Case Study

In this section, the IEEE 14-bus electric power system and an artificial 14-node natural gas transmission system are used for illustration purposes. Fig. 1 illustrates the structure of the combined system. The detailed data of the 14-node natural gas transmission system are shown in the Appendix.

Some modifications are applied to the IEEE 14-bus electric power system as follows: (1) the synchronous condensers at buses 3, 6, and 8 are replaced by distributed generators denoted G_3, G_6, and G_8; (2) the generators at buses 1 and 2 are assumed to be fired by natural gas; (3) the voltage upper and lower bounds are 1.06 and 0.94 pu.

The cost coefficients of each generator are shown in Tab.1. We assume that the costs of generators G_3, G_6, and G_8 are identical.

Table 1. Cost coefficients of generators

Generator	a_i^E [$/MW^{2}h]	b_i^E [$/MWh]	c_i^E [$/h]
G_1	0.043	20	100
G_2	0.25	20	100
G_3, G_6, G_8	0.01	40	50

The nodes of natural gas system are numbered using the same order of the electrical transmission system; see Fig.1. The entire natural gas transmission system is a looped structure with a gas well and a short-term storage, which can ensure the possibility to satisfy the $n-1$ criterion. Two compressor stations are installed in the natural gas system to regulate the pressure at pipelines 2-3 and 12-13, respectively. The power consumed by those compressor stations is directly purchased from the electric transmission system. The electricity price for all compressor stations is considered to be 0.05 $/kW·h.

According to the detailed data of the natural gas system, one can solve the nonlinear flow problem by Newton's method. With the PDIPA, the optimal dispatch solution (normal opera-

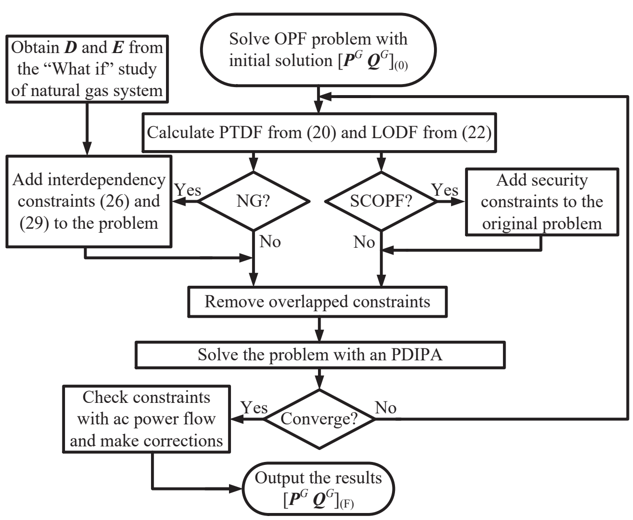

Fig. 3. Flowchart of interdependency based optimal power flow

Table 2. "What if" contingency analysis for the outage of pipeline 1-5

Case: 1-5 Outage	p_1^w [kpa]	F_8^I [Mm^3/day]	$r_{2,3}$	$r_{12,13}$	M^{NG} [$/s]	$P_{2,3}^E$ [MW]	$P_{12,13}^E$ [MW]
Normal	5000	0.4	1.17	1.16	30.67	1.55	1.57
Pre-redispatch	5000	0.4	1.17	1.16	31.17	2.48	2.10
Post-redispatch	5114	4.13	1.28	1.20	32.21	2.67	1.98

tion) is shown in the first row of Tab.2. To simulate the contingency scenario of the outage of pipeline 1-5, we follow the procedure pro-posed in Section 2.3. To illustrate the impact to the electric system generated by the natural gas system contingency, the system working statuses in the normal operation, pipeline outage contingency, and re-dispatch operation are shown in Fig.4. Tab.2 provides the corresponding "what if" analysis results. When the fault occurs, the natural gas system works with operating violations (pressure and gas flow violations occur), see Fig.4. The power consumptions of the compressor stations increase due to the increased flow rates. After the manager re-dispatches the natural gas system, the flow rate of the short-term storage FI8 and ratio of compressor stations are increased to force the system back to a safe operation. As a result, the electricity consumption of the compressor station $C_{2,3}$ further increases; see the electricity consumption variation in Tab.2.

Impact matrices **D** and **E** can be computed following the procedure proposed in Section 2.3. The electrical consumptions during the natural gas contingency after re-dispatching are shown in the Appendix. According to the "what if" studies, **D** is a zero matrix, meaning the generators can be connected to the natural gas system during the fault in natural gas system. The maximum power consumption of $CS_{2,3}$ is 2.67 MW and the maximum consumption of $CS_{12,13}$ is 2.61 MW based on matrix E. According to 27 and 30, two extra sets of interdependency constraints can be obtained.

New dispatch results can be found in Tab.3 after integrating the interdependency constraints into the OPF problem. The current upper bounds in the case are shown in Fig.5(b). The differences in the dispatch strategies and the operational cost of the electrical power system are very small. However, the robustness of the electrical power system increases substantially; see Fig.5. When a contingency scenario occurs in the interconnected natural gas system, say

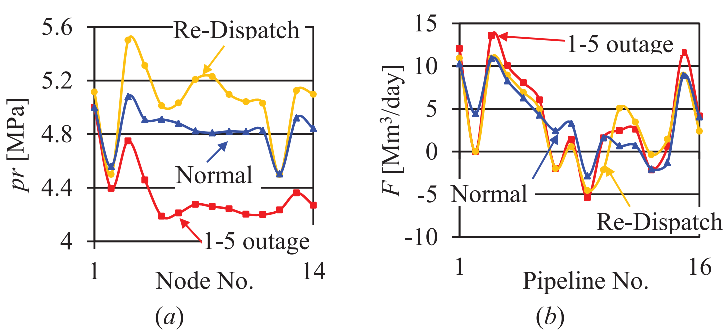

Fig. 4. Comparison between normal operation, post contingency, and re-dispatch results

pipeline 12-13 is out, the electricity consumptions of the compressor stations change. Correspondingly, two voltage violations occur in the electrical power system; see the dotted arrows in Fig.5(a). Meanwhile, there is a line current violation at branch 19 (transmission line 12-13); see the dotted arrow in Fig.5(b). When considering the PCIDIs, the burden on transmission lines 7-8 and 6-13 reduced under normal condition. Consequently, the two voltage violations are eliminated as well as the line current violation when the outage occurs.

The dispatch results of the IEEE 14-bus system are obtained solving the SCOPF problem with the interdependency constraints. Since the system parameters in the previous example cannot satisfy the $n-1$ criterion, we increased the capacities of the electrical transmission lines. Hence, the line current upper bounds, in this case, are adjusted to the line shown in Fig.6(b). The operational costs and their corresponding dispatch solutions (OPF problem, SCOPF problem, and SCOPF problem with interdependency constraints) can be found in Table 4. The behavior of the electric power system under those different scenarios can be seen in Figs.6 and 7, respectively. Comparing the operational cost for different dispatch re-

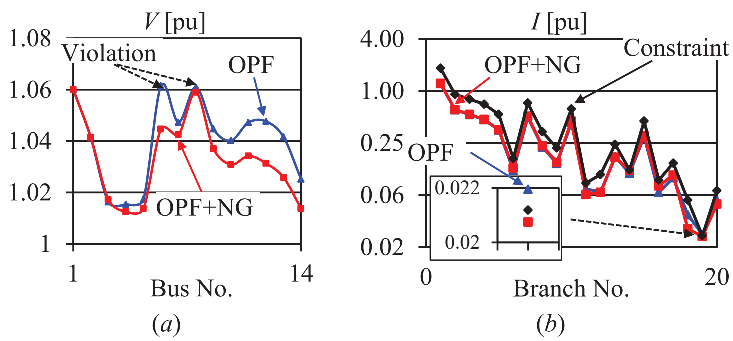

Fig. 5. Behavior of the electrical system after outage of pipeline 12-13 under OPF dispatch and proposed dispatch methods: (a) Voltage profile of the electrical system (b) Current profile of the electrical system

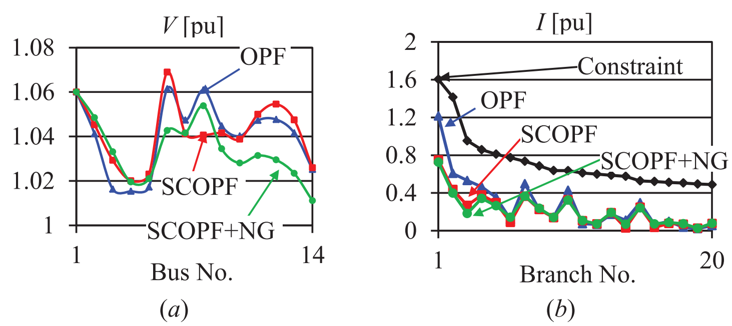

Fig. 6. Behavior of the electrical system following the outage of pipeline 12-13 under OPF dispatch, SCOPF dispatch, and proposed dispatch method: (a) Voltage profile of the electrical system (b) Current profile of the electrical system

Table 3. Solutions of different formulation without the consideration the contingency of the electrical power system

		G_1	G_2	G_3	G_6	G_8	M^E [k$/h]
OPF	MW	194.3	36.7	28.7	0	8.5	8.0815
	Mvar	0	23.7	24.1	11.5	8.3	
OPF+NG	MW	194.0	36.7	28.4	0	9.2	8.0821
	Mvar	0	25.9	25.2	8.0	8.8	

Table 4. Solutions of different formulation with the consideration the contingency of the electrical power system

		G_1	G_2	G_3	G_6	G_8	M^E [k$/h]
OPF	MW	194.3	36.7	28.7	0	8.5	8.08
	Mvar	0	23.7	24.1	11.5	8.3	
SCOPF	MW	127.1	41.8	75.6	16.4	3.0	8.37
	Mvar	6.4	14.4	17.0	12.7	-0.4	(+3.6%)
SCOPF+NG	MW	120.7	27.7	90.0	25.5	0	8.49
	Mvar	10	28.0	15.4	-5.3	7.3	(+5%)

sults, we can see that the operational cost of the OPF is the smallest. The operational costs of the SCOPF and proposed dispatch method increase 3.6% and 5%, respectively. However, the proposed dispatch method provides more robust systems than the OPF and SCOPF methods. When the outage of the pipeline 12-13 occurs, voltage violations happen when the electrical power system is dispatched based on the OPF and SCOPF solutions; see Fig.6(a). In contrast, the proposed dispatch method solves the voltage violation problems (see Fig.6(b)). When the worst contingency scenario (the outage of transmission line 1-2) in the electric power system occurs, the OPF dispatched system fails, and a blackout occurs. The proposed dispatched system not only prevents the blackout but also resolves the voltage profile problem and the line

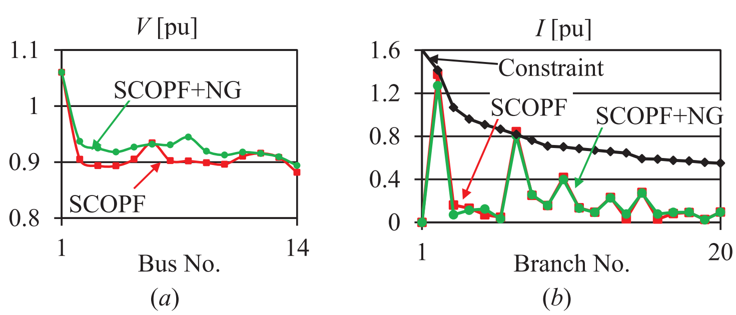

Fig. 7. Behaviour of the electrical system after the outage of transmission line 1-2 under SCOPF dispatch and proposed dispatch methods: (a) Voltage profile of the electrical system (b) Current profile of the electrical system

current violations; see Fig.7(b). Through the proposed analysis method, the system operator can make an intelligent choice between the operational cost and robustness of the systems.

5 Conclusion

A co-simulation platform has been proposed, and two impact matrices have been introduced to model the interdependency impacts from interconnected natural gas system to electric power system. To enhance the stability of the target electric power system and eliminate the impacts, interdependency constraints have been proposed to provide new dispatch options to the system operator. The IEEE 14-bus system paralleled with a natural gas transmission system, have been used to evaluate the impact of interdependencies and illustrate the advantages of the proposed interdependency constraints. The electrical power system has been found to be more robust when considering the interdependencies. It is worth pointing out that the solution of the interdependency analysis approach is more expensive than OPF and SCOPF. The proposed formulation integrates the existing models and provides a choice to utilities who aim to operate their systems more reliably in the presence of interdependencies with other systems.

Appendix

The electrical consumption data after re-dispatch are shown in Tab.5. The information on the buses of the artificial natural gas system is presented in Tab.6. The constant pressure node in the natural gas system is denoted as CP, and the constant flow rate node is denoted as CQ. The regular nodes are de-noted as L. All pipelines are assumed to have equal lengths of 80 km and equal inner diameters of 635 mm. The upper bounds of the pipeline are set to be 15 Mm3/day. The data of the sources in the natural gas system are provided in Tab.7.

Table 5. Electrical consumption data after re-dispatch

Contingency Scenario Pipeline index (from, to)	$P^E_{2,3}$ [MW]	$P^E_{12,13}$ [MW]	Contingency Scenario Pipeline index (from, to)	$P^E_{2,3}$ [MW]	$P^E_{12,13}$ [MW]
1. (1, 2)	fail	fail	09. (6, 13)	2.38	2.36
2. (1, 5)	2.67	1.98	10. (7, 8)	1.55	1.57
3. (1, 12)	fail	fail	11. (7, 9)	1.93	1.50
4. (2, 3)	0	1.29	12. (9, 10)	2.27	1.75
5. (3, 4)	0.26	1.18	13. (9, 14)	1.94	1.80
6. (4, 7)	0.65	1.15	14. (10, 11)	2.00	1.64
7. (5, 6)	2.67	2.15	15. (12, 13)	1.74	0
8. (6, 11)	1.66	1.59	16. (13, 14)	1.59	1.98

Table 6. Artificial 14-Bus natural gas system data sheet of buses

Bus No.	Bus Type	Load [$\mathrm{Mm}^3/\mathrm{day}$]	$[\underline{pr}, \overline{pr}]$ [kPa]
1	CP	2	[4500, 6000]
2 - 7	L	2	[4500, 6000]
8	CQ	2	[4500, 6000]
9 - 14	L	2	[4500, 6000]

Table 7. Artificial 14-Bus natural gas system data sheet of sources

Bus No.	Source Type	$[\underline{F}, \overline{F}]$ [$\mathrm{Mm}^3/\mathrm{day}$]	Price [\$/Btu]
1	CP	-	2.70
8	CQ	[0.4, 10]	3.71

References

1. MOHAMMAD Shahidehpour, Yong Fu, and Thomas Wiedman. Impact of natural gas infrastructure on electric power systems. *Proceedings of the IEEE*, 93(5):1042–1056, 2005.
2. Alberto Martinez-Mares and Claudio R Fuerte-Esquivel. A unified gas and power flow analysis in natural gas and electricity coupled networks. *IEEE Transactions on Power Systems*, 27(4):2156–2166, 2012.
3. Zhinong Wei, Sheng Chen, Guoqiang Sun, Dan Wang, Yonghui Sun, and Haixiang Zang. Probabilistic available transfer capability calculation considering static security constraints and uncertainties of electricity–gas integrated energy systems. *Applied Energy*, 167:305–316, 2016.
4. Tao Li, Mircea Eremia, and Mohammad Shahidehpour. Interdependency of natural gas network and power system security. *IEEE Transactions on Power Systems*, 23(4):1817–1824, 2008.
5. Moein Moeini-Aghtaie, Ali Abbaspour, Mahmud Fotuhi-Firuzabad, and Ehsan Hajipour. A decomposed solution to multiple-energy carriers optimal power flow. *IEEE Transactions on Power Systems*, 29(2):707–716, 2014.
6. Michele Arnold, Rudy R Negenborn, Goran Andersson, and Bart De Schutter. Model-based predictive control applied to multi-carrier energy systems. In *Power & Energy Society General Meeting, 2009. PES'09. IEEE*, pages 1–8. IEEE, 2009.
7. Xianjun Zhang, George G Karady, and Samuel T Ariaratnam. Optimal allocation of chp-based distributed generation on urban energy distribution networks. *IEEE Transactions on Sustainable Energy*, 5(1):246–253, 2014.
8. Nilufar Neyestani, Maziar Yazdani-Damavandi, Miadreza Shafie-Khah, Gianfranco Chicco, and João PS Catalão. Stochastic modeling of multienergy carriers dependencies in smart local networks with distributed energy resources. *IEEE Transactions on Smart Grid*, 6(4):1748–1762, 2015.
9. Xiaping Zhang, Mohammad Shahidehpour, Ahmed Alabdulwahab, and Abdullah Abusorrah. Hourly electricity demand response in the stochastic day-ahead scheduling of coordinated electricity and natural gas networks. *IEEE Transactions on Power Systems*, 31(1):592–601, 2016.

10. Ahmed Alabdulwahab, Abdullah Abusorrah, Xiaping Zhang, and Mohammad Shahidehpour. Stochastic security-constrained scheduling of coordinated electricity and natural gas infrastructures. *IEEE Systems Journal*, 2015.
11. Cong Liu, Mohammad Shahidehpour, Yong Fu, and Zuyi Li. Security-constrained unit commitment with natural gas transmission constraints. *IEEE Transactions on Power Systems*, 24(3):1523–1536, 2009.
12. Carlos M Correa-Posada and Pedro Sanchez-Martin. Security-constrained optimal power and natural-gas flow. *IEEE Transactions on Power Systems*, 29(4):1780–1787, 2014.
13. E Shashi Menon. *Gas pipeline hydraulics*. CRC Press, 2005.
14. Hongye Wang, Carlos E Murillo-Sanchez, Ray D Zimmerman, and Robert J Thomas. On computational issues of market-based optimal power flow. *IEEE Transactions on Power Systems*, 22(3):1185–1193, 2007.
15. Allen J Wood and Bruce F Wollenberg. *Power generation, operation, and control*. John Wiley & Sons, 2012.
16. Ray Daniel Zimmerman, Carlos Edmundo Murillo-Sánchez, and Robert John Thomas. Matpower: Steady-state operations, planning, and analysis tools for power systems research and education. *IEEE Transactions on power systems*, 26(1):12–19, 2011.
17. Brian Stott and Eric Hobson. Power system security control calculations using linear programming, part i. *IEEE Transactions on Power Apparatus and Systems*, (5):1713–1720, 1978.
18. James Jamal Thomas and Santiago Grijalva. Flexible security-constrained optimal power flow. *IEEE Transactions on Power Systems*, 30(3):1195–1202, 2015.
19. Wai Y Ng. Generalized generation distribution factors for power system security evaluations. *IEEE Transactions on Power Apparatus and Systems*, (3):1001–1005, 1981.
20. Teoman Guler, George Gross, and Minghai Liu. Generalized line outage distribution factors. *IEEE Transactions on Power Systems*, 22(2):879–881, 2007.
21. Tianqi Hong, Ashhar Raza, and Francisco de León. Optimal power dispatch under load uncertainty using a stochastic approximation method. *IEEE Transactions on Power Systems*, 31(6):4495–4503, 2016.